polymer papers

Analysis of orientation mechanism of crystallites in polyethylene cylindrical rod under tension–torsion combined stress

Takeshi Katagiri, Masanobu Sugimoto, Eiji Nakanishi* and Sadao Hibi
Department of Materials Science and Engineering, Nagoya Institute of Technology, Gokiso-cho, Showa-ku, Nagoya 466, Japan
(Received 20 January 1992; revised 21 August 1992)

A polyethylene cylindrical rod with lamellar structure is loaded with tension–torsion combined stress. The orientation behaviour of the crystallites is evaluated by an improved orientation distribution function. The function assumes affine deformation and that the orthogonal relation of the three crystallographic axes is maintained during deformation. The improved function is achieved by assuming that slippage deformation occurs in a crystallite block. For cases in which twist is strong and samples are highly deformed, the orientation behaviour is interpreted by taking into account the slippage deformation of the (1 1 0) plane. This, with the assumption of spiral orientation of the chain axis and rotation of the *a*- and *b*-axes around the *c*-axis, results in good agreement between calculation and experimental results.

(Keywords: polyethylene; combined stress; orientation distribution function; slippage deformation; pole figures; preferred orientation)

INTRODUCTION

The deformation mechanism of the crystalline texture of polyolefin with spherulitic structure has been studied by assuming affine deformation[1–5]. These studies focused on interlamellar and intralamellar deformations in a spherulite. Recently, Hibi *et al.*[6–9] have studied the deformation mechanism by an improved theory assuming orientation of the lattice axes. For large plastic deformation, the superstructures, such as spherulites, break down and are no longer suitable for use in analysing the orientation behaviour. Hibi's theory dealt with crystallite blocks smaller than a lamella and rotation of crystallite blocks accompanying plastic deformation was taken into account. With this improvement, the orientation behaviour of rolled sheet[6–8] and reorientation during off-angle drawing of rolled samples were evaluated[9].

In a previous paper[10], the authors have investigated the orientation behaviour of crystallites in a polyethylene cylindrical rod under tension–torsion combined stress by wide-angle X-ray diffraction (WAXD). As a result, it was suggested that the *c*-axis oriented in the apparent drawing direction and the *b*-axis oriented in the sample radial direction. To evaluate this orientation behaviour, the orientation distribution function proposed by Hibi[6–9] must be further improved because slippage of the crystallographic plane and spiral orientation of the chain axis both occurred under combined stress. The improvement will be made by assuming that rotation of the *a*- and *b*-axes around the *c*-axis occurs after the slippage deformation in a crystallite block. With these modifications, the orientation distribution function of crystallites and the *j*th individual crystallographic plane can be calculated. In this paper, the new orientation distribution function will be derived and the deformation mechanism under tension–torsion combined stress will be discussed. It is recommended that the previous paper[10] be referred to before proceeding further.

THEORY

The original idea of Hibi's theory is the assumption of affine deformation with volume kept constant and the orthogonal relation of the three crystallographic axes being maintained during plastic deformation. Two main factors are pointed out here as guidelines to the following derivation. First, under combined stress, the fact that the chain axis does not coincide with the cylinder axis of the specimen has to be considered in coordinate transformation. Second, the effect of rotation of the *a*- and *b*-axes around the *c*-axis due to slippage of the (1 1 0) plane will be complementary to the orientation distribution function of the main axes of crystallites.

Consideration of the spiral orientation

During deformation, the coordinate used to define the sample is not changed while the coordinate used to define the crystallite is affected by the resultant stress. Let the sample coordinate be defined as O–$X_1X_2X_3$ which has the X_1-axis as the radial axis, the X_2-axis as the circumference axis and the X_3-axis as the longitudinal axis. The corresponding unit vectors are $\boldsymbol{e}_1$, $\boldsymbol{e}_2$ and $\boldsymbol{e}_3$, respectively. On the other hand, the coordinate used to define the crystallite is set as the O–abc which has the *a*-, *b*- and *c*-axes corresponding to the crystallographic

* To whom correspondence should be addressed

0032-3861/93/122467-08

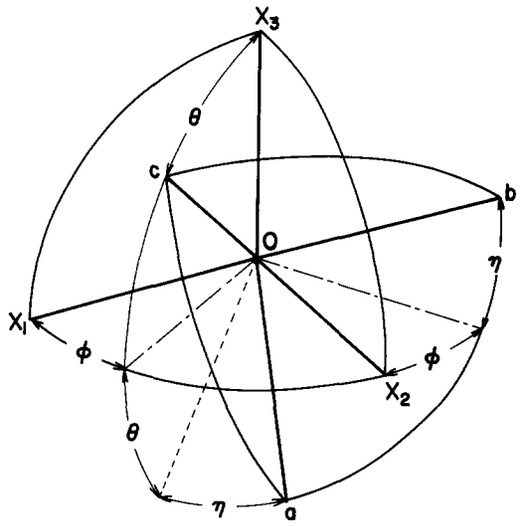

Figure 1 Eulerian angle θ, ϕ and η specifying the relation between the principal axis O–abc of the crystal and the Cartesian coordinates O–$X_1X_2X_3$

a-, b- and c-axes. The unit vectors of the latter system are $\boldsymbol{e}_a$, $\boldsymbol{e}_b$ and $\boldsymbol{e}_c$, respectively. These two systems are shown in *Figure 1*. The transformation which relates the O–abc to O–$X_1X_2X_3$ coordinates may be described in terms of three Eulerian angles, θ, ϕ and η, and is described as follows.

$$\begin{Bmatrix} e_1 \\ e_2 \\ e_3 \end{Bmatrix} = \begin{bmatrix} \cos\phi\cos\theta\cos\eta - \sin\phi\sin\eta, \\ \sin\phi\cos\theta\cos\eta + \cos\phi\sin\eta, \\ -\sin\theta\cos\eta \end{bmatrix}$$
$$\begin{matrix} -\cos\phi\cos\theta\sin\eta - \sin\phi\cos\eta, & \sin\theta\cos\phi \\ -\sin\phi\cos\theta\sin\eta + \cos\phi\cos\eta, & \sin\theta\sin\phi \\ \sin\theta\sin\eta, & \cos\theta \end{matrix} \begin{Bmatrix} e_a \\ e_b \\ e_c \end{Bmatrix}$$
$$= \begin{bmatrix} a_{11}, & a_{12}, & a_{13} \\ a_{21}, & a_{22}, & a_{23} \\ a_{31}, & a_{32}, & a_{33} \end{bmatrix} \begin{Bmatrix} e_a \\ e_b \\ e_c \end{Bmatrix} \quad (1)$$

It has been proved in the previous paper[10] that, when the polyethylene cylindrical rod was loaded with tension–torsion combined stress, the c-axis, which is the molecular axis, oriented in the direction of tilting from the sample axis, due to the resultant force of tensile and shear forces. The tilt angle is defined as the spiral angle β. The tilting direction, which is the apparent draw direction, is here defined as the X'_3-axis. Let the X_1-axis be kept unchanged and then the X'_2-axis is defined as the axis perpendicular to the X'_3–X_1 plane. The unit vectors after deformation then become e'_1, e'_2 and e'_3. Transformation from the O–$X_1X_2X_3$ to O–$X'_1X'_2X'_3$ ($X'_1 = X_1$) coordinates may be described by the following equation:

$$\begin{Bmatrix} e'_1 \\ e'_2 \\ e'_3 \end{Bmatrix} = \begin{bmatrix} 1, & 0, & 0 \\ 0, & \cos\beta, & \sin\beta \\ 0, & -\sin\beta, & \cos\beta \end{bmatrix} \begin{Bmatrix} e_1 \\ e_2 \\ e_3 \end{Bmatrix} \quad (2)$$

Until this point, relation of the O–abc and the O–$X'_1X'_2X'_3$ coordinates can be established. Because the cylindrical rod has a curvature and the specimens prepared for X-ray measurement were cut from the deformed rods, one more modification is necessary to correct the X-ray incident angle so that simulation can be close to the real condition. This correction is expressed by the following equation described in terms of the correction angle δ around the X'_3-axis:

$$\begin{Bmatrix} e''_1 \\ e''_2 \\ e''_3 \end{Bmatrix} = \begin{bmatrix} \cos\delta, & \mp\sin\delta, & 0 \\ \pm\sin\delta, & \cos\delta, & 0 \\ 0, & 0, & 1 \end{bmatrix} \begin{Bmatrix} e'_1 \\ e'_2 \\ e'_3 \end{Bmatrix} \quad (3)$$

When the cylindrical rod is loaded with tension–torsion combined stress, the relation of the Cartesian coordinate O–abc of the crystallite with respect to the reference coordinate O–$X''_1X''_2X''_3$ of the bulk sample can be derived from the foregoing discussion. The relative positions before deformation of the crystallite axes and reference axes are summarized in *Figure 2* and are expressed in the following equation:

$$\begin{Bmatrix} e''_1 \\ e''_2 \\ e''_3 \end{Bmatrix} = \begin{bmatrix} \cos\delta, & \mp\sin\delta, & 0 \\ \pm\sin\delta, & \cos\delta, & 0 \\ 0, & 0, & 1 \end{bmatrix} \begin{bmatrix} 1, & 0, & 0 \\ 0, & \cos\beta, & \sin\beta \\ 0, & -\sin\beta, & \cos\beta \end{bmatrix}$$
$$\times \begin{bmatrix} \cos\phi\cos\theta\cos\eta - \sin\phi\sin\eta, \\ \sin\phi\cos\theta\cos\eta + \cos\phi\sin\eta, \\ -\sin\theta\cos\eta, \end{bmatrix}$$
$$\begin{matrix} -\cos\phi\cos\theta\sin\eta - \sin\phi\cos\eta, & \sin\theta\cos\phi \\ -\sin\phi\cos\theta\sin\eta + \cos\phi\cos\eta, & \sin\theta\sin\phi \\ \sin\theta\sin\eta, & \cos\theta \end{matrix} \begin{Bmatrix} e_a \\ e_b \\ e_c \end{Bmatrix}$$
$$= \begin{bmatrix} \cos\phi^*\cos\theta^*\cos\eta^* - \sin\phi^*\sin\eta^*, \\ \sin\phi^*\cos\theta^*\cos\eta^* + \cos\phi^*\sin\eta^*, \\ -\sin\theta^*\cos\eta^*, \end{bmatrix}$$
$$\begin{matrix} -\cos\phi^*\cos\theta^*\sin\eta^* - \sin\phi^*\cos\eta^*, & \sin\theta^*\cos\phi^* \\ -\sin\phi^*\cos\theta^*\sin\eta^* + \cos\phi^*\cos\eta^*, & \sin\theta^*\sin\phi^* \\ \sin\theta^*\sin\eta^*, & \cos\theta^* \end{matrix} \begin{Bmatrix} e_a \\ e_b \\ e_c \end{Bmatrix}$$
$$= \begin{bmatrix} a^*_{11}, & a^*_{12}, & a^*_{13} \\ a^*_{21}, & a^*_{22}, & a^*_{23} \\ a^*_{31}, & a^*_{32}, & a^*_{33} \end{bmatrix} \begin{Bmatrix} e_a \\ e_b \\ e_c \end{Bmatrix} \quad (4)$$

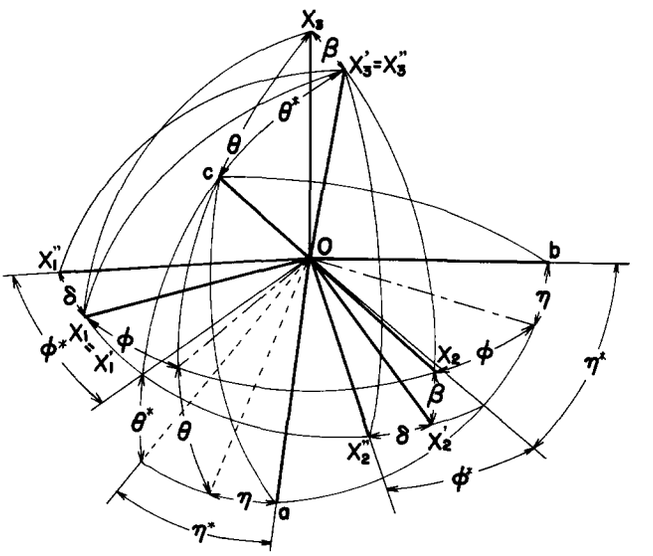

Figure 2 Eulerian angles θ^*, ϕ^* and η^* specifying the relation between the coordinates O-abc and O-$X''_1X''_2X''_3$. The spiral angle β and the correction angle δ specifying the relation between the coordinates O-$X_1X_2X_3$ and O-$X''_1X''_2X''_3$

Orientation distribution function of the crystallite axes

With the coordinate system expressed in equation (4) and shown in *Figure 2*, the orientation distribution function will be derived without taking into account the slippage deformation at this moment. The slippage deformation will be explained later. The assumptions made are affine deformation and the orthogonal relation of the three lattice axes.

As mentioned above, when the cylindrical rod was loaded with tension–torsion combined stress, the apparent drawing direction did not coincide with the sample axis direction. The orientation behaviour is analysed by using the reference coordinate, O–$X_1''X_2''X_3''$, as the coordinate system after deformation. The relation between the crystallite and the reference O–$X_1''X_2''X_3''$ coordinate as shown in equation (4) can be expressed by the azimuthal angle ϕ^*, the polar angle θ^* and the rotational angle η^*. To define the c-axis in the O–$X_1''X_2''X_3''$ system, angles ϕ^* and θ^* are sufficient, while the a- and b-axes depend on both the c-axis direction and the rotational angle η^*. The orientation distribution function of crystallites before deformation, $w^*(\cos\theta^*, \phi^*, \eta^*)$, is expressed as the probability density function with respect to the $\boldsymbol{a}$, $\boldsymbol{b}$ and $\boldsymbol{c}$ vectors.

After deformation, the relation between the O–$X_1''X_2''X_3''$ and O–abc coordinates is expressed in terms of the new Eulerian angle $\theta^{*\prime}$, $\phi^{*\prime}$ and $\eta^{*\prime}$, and the orientation distribution function becomes $w^{*\prime}(\cos\theta^{*\prime}, \phi^{*\prime}, \eta^{*\prime})$. In the following text, the deformed system is represented by symbols with superscript $'$. The relation of the orientation distribution function before and after deformation can be expressed as:

$$w^{*\prime}(\cos\theta^{*\prime}, \phi^{*\prime}, \eta^{*\prime}) = w^*(\cos\theta^*, \phi^*, \eta^*)\frac{\sin\theta^*\,\mathrm{d}\theta^*\,\mathrm{d}\phi^*\,\mathrm{d}\eta^*}{\sin\theta^{*\prime}\,\mathrm{d}\theta^{*\prime}\,\mathrm{d}\phi^{*\prime}\,\mathrm{d}\eta^{*\prime}} \tag{5}$$

The function is expressed in terms of change of the ratio of the polar angle, the azimuthal angle and the rotational angle before and after deformation.

It is assumed that the deformation is uniform throughout the sample and deformation ratios in the X_1'', X_2'' and X_3'' direction are λ_1, λ_2 and λ_3, respectively. The $\boldsymbol{c}$ vector of the c-axis direction became the $\boldsymbol{c}'$ vector by affine deformation and the $\boldsymbol{a}$ and $\boldsymbol{b}$ vectors became the $\boldsymbol{a}'$ and $\boldsymbol{b}'$ vectors, keeping the orthogonal relation to the $\boldsymbol{c}$ vector, respectively. Consequently the X_1'', X_2'' and X_3'' components of the $\boldsymbol{c}$ vector become λ_1, λ_2 and λ_3 times, and those of the $\boldsymbol{a}$ and $\boldsymbol{b}$ vectors become λ_{1a}, λ_{2a}, λ_{3a}, λ_{1b}, λ_{2b} and λ_{3b} times, respectively. Here, the relation between λ_i and λ_{ib} can be expressed using the following equations, by assuming that constant volume and the orthogonal relation of the three axes are maintained:

$$\lambda_1\lambda_{1b} = \lambda_2\lambda_{2b} = \lambda_3\lambda_{3b} = 1$$
$$\lambda_1\lambda_2\lambda_3 = 1$$
$$\lambda_{1b}\lambda_{2b}\lambda_{3b} = 1$$

The derivation of these relations is shown in a previous paper[6].

Next, the orientation distribution function of crystallites after deformation, $w^{*\prime}(\cos\theta^{*\prime}, \phi^{*\prime}, \eta^{*\prime})$, is derived in terms of the deformed ratios λ_1, λ_2 and λ_3. Let the length of the $\boldsymbol{c}$ vector before and after deformation be r_c and r_c', respectively. The change in ratios of the polar angle and the azimuthal angle are expressed in terms of the change in length of the $\boldsymbol{c}$ vector as:

$$\left(\frac{r_c'}{r_c}\right)^3 = \frac{\sin\theta^*\,\mathrm{d}\theta^*\,\mathrm{d}\phi^*}{\sin\theta^{*\prime}\,\mathrm{d}\theta^{*\prime}\,\mathrm{d}\phi^{*\prime}} \tag{6}$$

The relation of the $\boldsymbol{c}$ vector components (in the O–$X_1''X_2''X_3''$ coordinate system) before and after deformation is expressed as:

$$r_c\begin{Bmatrix}\lambda_1(a_{13}^*)\\ \lambda_2(a_{23}^*)\\ \lambda_3(a_{33}^*)\end{Bmatrix} = r_c'\begin{Bmatrix}a_{13}^{*\prime}\\ a_{23}^{*\prime}\\ a_{33}^{*\prime}\end{Bmatrix}$$

Because $(a_{13}^*)^2 + (a_{23}^*)^2 + (a_{33}^*)^2 = 1$ in Cartesian coordinates, this leads to:

$$(r_c'/r_c)^2 = 1/C_1$$
$$C_1 = (a_{13}^{*\prime}/\lambda_1)^2 + (a_{23}^{*\prime}/\lambda_2)^2 + (a_{33}^{*\prime}/\lambda_3)^2 \tag{7}$$

The $\boldsymbol{c}'$ vector is therefore further described in the next equation:

$$(a_{13}^{*\prime})^2 = C_1\lambda_1^2(a_{13}^*)^2 \tag{8a}$$
$$(a_{23}^{*\prime})^2 = C_1\lambda_2^2(a_{23}^*)^2 \tag{8b}$$
$$(a_{33}^{*\prime})^2 = C_1\lambda_3^2(a_{33}^*)^2 \tag{8c}$$

Substituting equation (4) into equation (7) leads to:

$$(r_c'/r_c) = C_1^{-1/2}$$
$$= \lambda_1\lambda_3[\lambda_1^2\cos^2\theta^{*\prime} + \lambda_3^2\sin^2\theta^{*\prime}(\cos^2\phi^{*\prime} + \lambda_1^4\lambda_3^2\sin^2\phi^{*\prime})]^{1/2} \tag{9}$$

Therefore, as C_1 can be determined from equation (7), the vector $\boldsymbol{c}'$ can be derived from equation (8) and the chain axis of the crystallite is defined.

To define the orientation of the main axes of the crystallite, one more axis has to be defined. The change of the $\boldsymbol{b}$ vector due to deformation is considered by leading the change ratio of the rotational angle η^*. As the length of the $\boldsymbol{b}$ vector changes from r_b to r_b':

$$r_b\begin{Bmatrix}\lambda_{1b}(a_{12}^*)\\ \lambda_{2b}(a_{22}^*)\\ \lambda_{3b}(a_{32}^*)\end{Bmatrix} = r_b'\begin{Bmatrix}a_{12}^{*\prime}\\ a_{22}^{*\prime}\\ a_{32}^{*\prime}\end{Bmatrix} \tag{10}$$

From the second and third rows of equation (10):

$$\frac{a_{22}^{*\prime}}{a_{32}^{*\prime}} = \frac{\lambda_{2b}(a_{22}^*)}{\lambda_{3b}(a_{32}^*)} \tag{11}$$

Substituting equation (4) into equation (11) leads to:

$$-\sin\phi^{*\prime}\cos\theta^{*\prime} + \cos\phi^{*\prime}\cos\eta^{*\prime}/\sin\eta^{*\prime}$$
$$= (\lambda_{2b}/\lambda_{3b})(\sin\theta^{*\prime}/\sin\theta^*)$$
$$\times(-\sin\phi^*\cos\theta^* + \cos\phi^*\cos\eta^*/\sin\eta^*) \tag{12}$$

Differentiating equation (12) with respect to η^* and $\eta^{*\prime}$, one obtains:

$$\mathrm{d}\eta^*/\mathrm{d}\eta^{*\prime} = (\cos\phi^{*\prime}/\cos\phi^*)(\sin\eta^*/\sin\eta^{*\prime})^2$$
$$\times(\lambda_{3b}/\lambda_{2b})(\sin\theta^*/\sin\theta^{*\prime}) \tag{13}$$

In equation (13), θ^*, ϕ^* and η^* denote the undeformed state. In order to deal only with angles after deformation, further treatment is necessary and the derivation is summarized in a previous paper[6]. Only the result is shown

here:

$$d\eta^*/d\eta^{*\prime} = \lambda_{1b}\lambda_1 C_1^{1/2} B_1^{-1}$$

$$B_1 = (a_{12}^{*\prime}/\lambda_{1b})^2 + (a_{22}^{*\prime}/\lambda_{2b})^2 + (a_{32}^{*\prime}/\lambda_{3b})^2 \quad (14)$$

In this way, the change of the $\theta^{*\prime}$, $\phi^{*\prime}$ and $\eta^{*\prime}$ with respect to the θ^*, ϕ^* and η^* is expressed in terms of the values of the deformed state so that the orientation distribution function after deformation can be obtained. Substituting equations (6), (9) and (14) into equation (5), one obtains:

$$w^{*\prime}(\cos\theta^{*\prime}, \phi^{*\prime}, \eta^{*\prime}) = w^*(\cos\theta^*, \phi^*, \eta^*)\lambda_{1b}\lambda_1 B_1^{-1} C_1^{-1} \quad (15)$$

As the material before deformation is considered to be without orientation, the $w^*(\cos\theta^*, \phi^*, \eta^*)$ in equation (15) can be replaced with a constant. The orientation distribution function of crystallites, $w^{*\prime}(\cos\theta^{*\prime}, \phi^{*\prime}, \eta^{*\prime})$, in equation (15) is based on the reference coordinate O–$X_1''X_2''X_3''$ as shown in *Figure 2*.

Slippage deformation of the (1 1 0) plane

As mentioned previously, at large deformation the slippage of the (1 1 0) plane is followed by rotation of the *a*- and *b*-axes around the *c*-axis. Let α be the rotational angle due to such slippage. Then, the relation between the coordinates used to define the unit cell before slippage (*O–abc*) and after slippage (O-$a^\# b^\# c^\#$) can be shown schematically as in *Figure 3*. Let the unit vectors in the O-$a^\# b^\# c^\#$ system be $\boldsymbol{e}_a^\#$, $\boldsymbol{e}_b^\#$ and $\boldsymbol{e}_c^\#$, and *Figure 3* can be numerically presented as:

$$\begin{Bmatrix} \boldsymbol{e}_a \\ \boldsymbol{e}_b \\ \boldsymbol{e}_c \end{Bmatrix} = \begin{bmatrix} \cos\alpha, & -\sin\alpha, & 0 \\ \sin\alpha, & \cos\alpha, & 0 \\ 0, & 0, & 1 \end{bmatrix} \begin{Bmatrix} \boldsymbol{e}_a^\# \\ \boldsymbol{e}_b^\# \\ \boldsymbol{e}_c^\# \end{Bmatrix} \quad (16)$$

Substituting equation (16) into equation (4), one obtains:

$$\begin{Bmatrix} \boldsymbol{e}_1'' \\ \boldsymbol{e}_2'' \\ \boldsymbol{e}_3'' \end{Bmatrix} = \begin{bmatrix} \cos\phi^*\cos\theta^*\cos\eta^* - \sin\phi^*\sin\eta^*, \\ \sin\phi^*\cos\theta^*\cos\eta^* + \cos\phi^*\sin\eta^*, \\ -\sin\theta^*\cos\eta^* \end{bmatrix}$$

$$\begin{matrix} -\cos\phi^*\cos\theta^*\sin\eta^* - \sin\phi^*\cos\eta^*, & \sin\theta^*\cos\phi^* \\ -\sin\phi^*\cos\theta^*\sin\eta^* + \cos\phi^*\cos\eta^*, & \sin\theta^*\sin\phi^* \\ \sin\theta^*\sin\eta^*, & \cos\theta^* \end{matrix} \Bigg]$$

$$\times \begin{bmatrix} \cos\alpha, & -\sin\alpha, & 0 \\ \sin\alpha, & \cos\alpha, & 0 \\ 0, & 0, & 1 \end{bmatrix} \begin{Bmatrix} \boldsymbol{e}_a^\# \\ \boldsymbol{e}_b^\# \\ \boldsymbol{e}_c^\# \end{Bmatrix}$$

$$= \begin{bmatrix} \cos\phi^\#\cos\theta^\#\cos\eta^\# - \sin\phi^\#\sin\eta^\#, \\ \sin\phi^\#\cos\theta^\#\cos\eta^\# + \cos\phi^\#\sin\eta^\#, \\ -\sin\theta^\#\cos\eta^\#, \end{bmatrix}$$

$$\begin{matrix} -\cos\phi^\#\cos\theta^\#\sin\eta^\# - \sin\phi^\#\cos\eta^\#, & \sin\theta^\#\cos\phi^\# \\ -\sin\phi^\#\cos\theta^\#\sin\eta^\# + \cos\phi^\#\cos\eta^\#, & \sin\theta^\#\sin\phi^\# \\ \sin\theta^\#\sin\eta^\#, & \cos\theta^\# \end{matrix} \Bigg] \begin{Bmatrix} \boldsymbol{e}_a^\# \\ \boldsymbol{e}_b^\# \\ \boldsymbol{e}_c^\# \end{Bmatrix}$$

$$= \begin{bmatrix} a_{11}^\#, & a_{12}^\#, & a_{13}^\# \\ a_{21}^\#, & a_{22}^\#, & a_{23}^\# \\ a_{31}^\#, & a_{32}^\#, & a_{33}^\# \end{bmatrix} \begin{Bmatrix} \boldsymbol{e}_a^\# \\ \boldsymbol{e}_b^\# \\ \boldsymbol{e}_c^\# \end{Bmatrix} \quad (17)$$

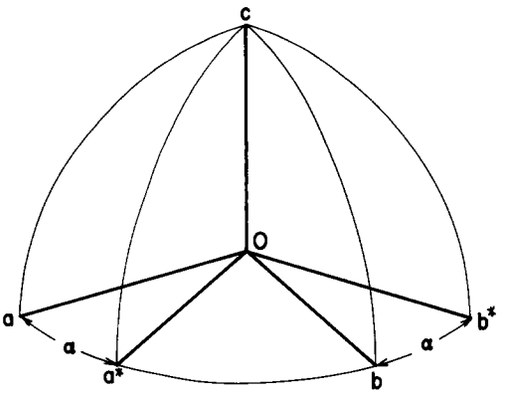

Figure 3 Rotation of the principal axis *O–abc* around the *c*-axis for slippage in the crystallite block

In this way, the coordinate system of the crystallite after deformation is related to the coordinate system used in the experiment. This enables direct comparison to be made between the calculated and the experimental results.

Orientation distribution function of crystal plane

Next, the orientation distribution function of the *j*th individual crystal plane, $q^j(\cos\theta_j, \phi_j)$, will be derived. The orientation distribution function of crystallites, after considering the spiral orientation and slippage deformation, is denoted as $w'(\cos\theta', \phi', \eta')$. Derivation of the $w'(\cos\theta', \phi', \eta')$ function can be performed easily as shown in equation (15), and may be expanded into the equation shown below through the expansion of Jacobi's polynomials up to the expansion coefficient $l = 8$:

$$w'(\cos\theta', \phi', \eta') = \sum_{l=0}^{8}\sum_{m=-l}^{l}\sum_{n=-l}^{l} [A_{lmn}\cos(m\phi' + n\eta') + B_{lmn}\sin(m\phi' + n\eta')] Z_{lmn}(\cos\theta') \quad (18)$$

where the coefficients A_{lmn} and B_{lmn} may be given as:

$$\begin{Bmatrix} A_{lmn} \\ B_{lmn} \end{Bmatrix} = \frac{1}{4\pi^2}\int_{\eta'=0}^{2\pi}\int_{\phi'=0}^{2\pi}\int_{\theta'=0}^{2\pi} w'(\cos\theta', \phi', \eta') \times \begin{Bmatrix} \cos(m\phi' + n\eta') \\ \sin(m\phi' + n\eta') \end{Bmatrix} Z_{lmn}(\cos\theta')\sin\theta'\, d\theta'\, d\phi'\, d\eta' \quad (19)$$

With these two values, A_{lmn} and B_{lmn}, the orientation distribution function of the *j*th individual crystal plane may be expanded as:

$$q^j(\cos\theta_j, \phi_j) = \sum_{l=0}^{8}\sum_{m=-l}^{l} [A_{lm}^j\cos(m\phi_j) + B_{lm}^j\sin(m\phi_j)] \prod_l^m(\cos\theta_j) \quad (20)$$

Here, the polar angle θ_j and the azimuthal angle ϕ_j link the crystal plane normal r_j with the Cartesian coordinate O–$X_1X_2X_3$. The coefficients A_{lmn} and B_{lmn} in equation (19) may be related to A_{lm}^j and B_{lm}^j in equation (20) in terms of the addition theorem of Legendre polynomials:

$$\begin{Bmatrix} A_{lm}^j \\ B_{lm}^j \end{Bmatrix} = 2\pi\left(\frac{2}{2l+1}\right)^{1/2} \times \sum_{m=-l}^{l} \begin{Bmatrix} A_{lmn}\cos(n\Phi_j) - B_{lmn}\sin(n\Phi_j) \\ A_{lmn}\sin(n\Phi_j) + B_{lmn}\cos(n\Phi_j) \end{Bmatrix} \prod_l^n(\cos\Theta_j) \quad (21)$$

Table 1 Conditions for the combined stress loading experiments

Notation	Tensile speed (mm min^{-1})	Torsional speed (deg min^{-1})
Tension	0.5	–
A	0.5	8
B	0.5	15
C	0.5	25
Torsion	–	15

Table 2 Draw ratio of each sample

	Tension	A	B	C	Torsion
Draw ratio	9.0	10.5	11.0	11.0	3.4

Table 3 Correctional angles of each sample

	Tension	A	B	C	Torsion
Correction angle, δ (degree)	0.0	0.0	4.2	6.5	11.5
Spiral orientation angle, β (degree)	0.0	23.0	42.0	55.0	75.0
Slippage angle, α (degree)	0.0	0.0	10.0	15.0	0.0

$\prod_l^m(\cos\theta_j)$ and $\prod_l^n(\cos\Theta_j)$ are the associated Legendre polynomials, which may be further related to the Legendre polynomials as follows:

$$Z_{l0_n}(\cos\Theta_j)=\prod_l^n(\cos\Theta_j) \quad (22)$$

$$Z_{lm0}(\cos\theta_j)=\prod_l^m(\cos\theta_j) \quad (23)$$

The polar angle Θ_j and the azimuthal angle Φ_j link the crystal plane normal r_j with the Cartesian coordinate O–abc. The coefficients A_{lm}^j and B_{lm}^j in equation (21) are given in terms of each jth crystal plane. In this paper, substituting the coefficients about the (1 1 0), (2 0 0), (0 2 0) and (0 0 2) planes into equation (20) leads to the four orientation distribution functions of the crystal plane normal. Then, the pole figures calculated by these functions are compared with the measured pole figures of the corresponding crystal plane.

EXPERIMENTAL

The samples for WAXD, which were the same as in the previous paper[10], were prepared as rectangular chips by sliding off the surface of the deformed polyethylene cylindrical rod. These chips were then arranged into a small plate with the aid of amorphous silicon adhesive. The conditions of the combined stress are summarized in *Table 1*. The draw ratios of the bulk samples are shown in *Table 2*. The correction angle δ of each condition mentioned above is shown in *Table 3*. The instrument used was a Rigaku X-ray generator (CN2028) equipped with pole figure attachment (PMG-A2) at 40 kV and 20 mA. A CuKα X-ray and Ni filter was used.

RESULTS AND DISCUSSION

Figure 4 shows the pole figures measured from WAXD. Each normal of the (1 1 0), (2 0 0) and (0 2 0) planes of the uniaxially drawn sample in *Figure 4a* distributes randomly in the X_1–X_2 plane and does not show any concentration as a peak. On the other hand, in cases of the simply twisted sample and the combined stressed samples, these normals distribute in the plane rotated from the X_1–X_2 plane toward the X_1–X_3 plane, and peaks appear, showing the concentration. The angle between the X_1–X_2 plane and the concentration peak is defined as the spiral orientation angle β, values of which are shown in *Table 3*.

Simulation without considering slippage deformation

Figure 5 shows the pole figures calculated by the orientation distribution function of the normals of the jth individual crystal plane, $q^j(\cos\theta_j, \phi_j)$. In the calculation, the correction angle δ and the spiral orientation angle β in *Table 3* were used. In the uniaxially drawn sample, the normal of the (0 0 2) plane, which represents the c-axis, orients strongly in the X_3-axis direction. The intensity distribution in the calculated pole figures of the simply twisted sample are similar to the pole figures shown in *Figure 4b*, and the (0 2 0) plane normal, showing the orientation of the b-axis, orients selectively in the X_1-axis direction which is the sample radial direction. In *Figure 5c*, the intensity distribution is qualitatively in accord with the pole figures, showing that the (0 0 2) plane normal orients strongly in the apparent drawing direction. As mentioned in the Introduction, the orientation distribution function is regarded as originating from the rotation of crystallite blocks that subdivided from a lamella. For uniaxial tensile, simple twist and condition A, it is suggested that a lamella broke due to the resultant force of the applied combined loading and the resulting crystallite blocks rearrange such that the normal of the (0 0 2) plane points to the apparent drawing direction. In addition, it is suggested that non-uniform stress distribution existed inside the sample cross-sectional plane and this resulted in the rotation of the major axis of the crystallite towards the sample radial direction.

For conditions B and C, the maximum intensity position of the (1 1 0) plane normal and its intensity distribution are somewhat different from those of the measured pole figures. Considering the crystal unit cell of polyethylene, the normals of the (1 1 0), (2 0 0) and (0 2 0) planes lie in the same plane, and the angle between the normal of the (1 1 0) plane and that of the (0 2 0) plane is 33.7° (ref. 11). In condition A, the angle between the peak positions of these two normals is greater than 30°, while for conditions B and C it is less than 30°. The spread of the intensity distribution becomes sharper in the azimuthal direction and broader in the polar direction.

Simulation with slippage deformation

The discrepancy between the calculation and the measurement in the previous subsection is suggested to be due to the slippage deformation of the (1 1 0) plane, as mentioned previously. It is thought that deformation, including a rotation of the a- and b-axes around the c-axis, must occur in conditions in which twist is strong. This rotation is considered to be due to slippage of the (1 1 0) plane which is the most closely packed atomic plane of polyethylene. A simple schematic representation of such a mechanism is shown in *Figure 6*. When the slippage deformation and rotation mechanisms occur, the normals of the (1 1 0), (2 0 0) and (0 2 0) planes turn around

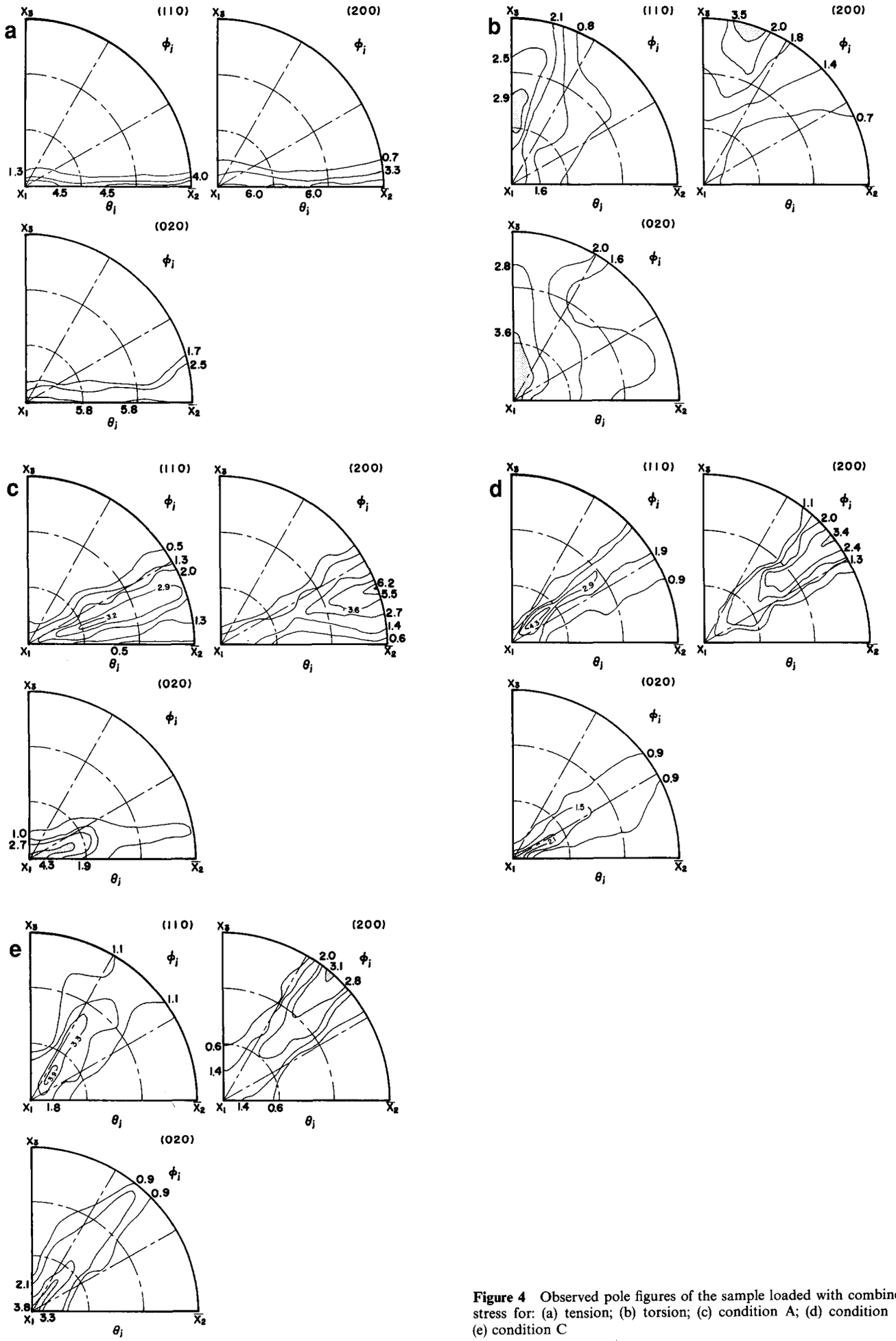

Figure 4 Observed pole figures of the sample loaded with combined stress for: (a) tension; (b) torsion; (c) condition A; (d) condition B; (e) condition C

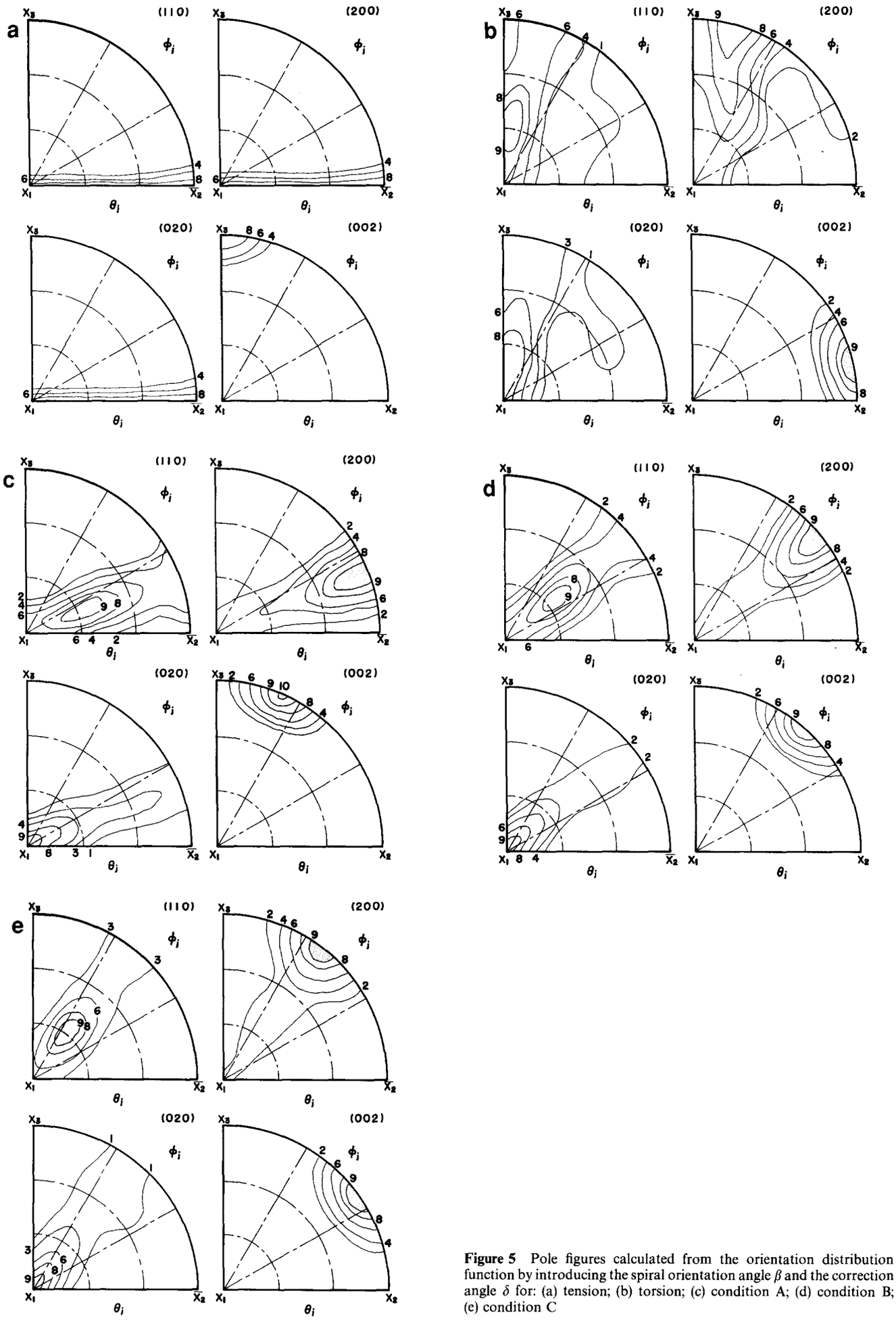

Figure 5 Pole figures calculated from the orientation distribution function by introducing the spiral orientation angle β and the correction angle δ for: (a) tension; (b) torsion; (c) condition A; (d) condition B; (e) condition C

the c-axis. This is illustrated in *Figure 3* and expressed in equation (16). The values of the slippage angle α that are obtained from the measured pole figures are summarized in *Table 3*. The calculated pole figures, in which α is considered, are shown in *Figure 7*. The maximum intensity area of the (1 1 0) plane normal shifts to the direction with smaller polar angle, and the intensity distribution of the (1 1 0), (2 0 0) and (0 2 0) plane normals becomes broader. The calculated pole figures are qualitatively in accord with the measured pole figures. It is suggested that, when crystallite blocks that subdivided from a lamella rearrange, the slippage deformation occurs in the direction perpendicular to the c-axis on the (1 1 0) plane in the crystallite block because of the twisting effect in the combined stress in conditions in which twist is strong.

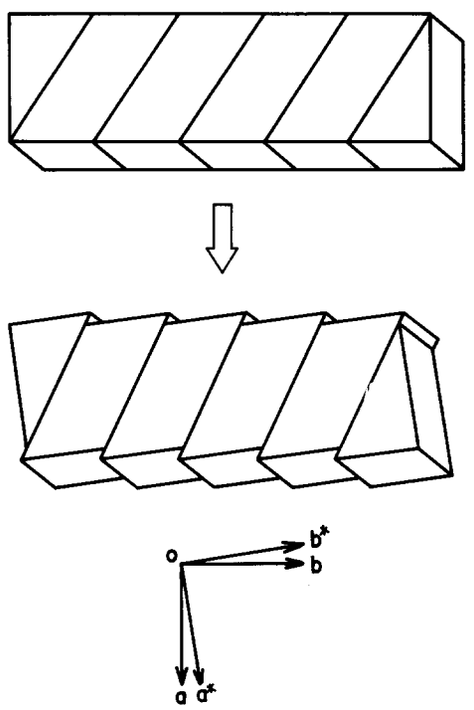

Figure 6 Schematic illustration of the slippage deformation on the (1 1 0) plane and rotation of the a- and b-axes around the c-axis in the crystallite block

CONCLUSIONS

From the above results and discussion, the following conclusions may be drawn about the deformation mechanism of a polyethylene cylindrical rod under tension–torsion combined stress.

When the cylindrical rod is loaded with combined stress under strong tensile or a small ratio of deformation, it is suggested that rearrangement of crystallite blocks occurs due to the resultant force of tension and shear forces. The c-axis orients in the direction of the resultant force while the b-axis orients in the radial direction.

When twist is strong and the sample is highly deformed, it is suggested that the slippage deformation occurs in the direction perpendicular to the c-axis on the (1 1 0) plane, and the a- and b-axes rotate around the c-axis in the crystallite block.

REFERENCES

1 Sasaguri, K., Hoshino, S. and Stein, R. S. *J. Appl. Phys.* 1964, **35**, 47
2 Sasaguri, K., Yamada, R. and Stein, R. S. *J. Appl. Phys.* 1964, **35**, 3188
3 Oda, T., Nomura, S. and Kawai, H. *J. Polym. Sci. A* 1965, **3**, 1993
4 Takahara, H. and Kawai, H. *Senn-i Gakkaishi* 1968, **24**, 311
5 Moore, K. S. *J. Polym. Sci., A-2* 1967, **5**, 711
6 Hibi, S., Maeda, M., Yokoyama, A., Fujita, K. and Kurata, N. *Kobunshi Ronbunshu* 1985, **42**, 63
7 Suzuki, K., Hibi, S., Torii, T., Kobayashi, A., Nakanishi, E. and Maeda, M. *Kobunshi Ronbunshu* 1987, **44**, 491
8 Hibi, S., Suzuki, H., Hirano, T., Torii, T., Fujita, K., Nakanishi, E. and Maeda, M. *Kobunshi Ronbunshu* 1988, **45**, 237
9 Torii, T., Hibi, S., Kodama, E., Nakanishi, E., Maeda, M. and Fujimoto, K. *Kobunshi Ronbunshu* 1987, **44**, 503
10 Katagiri, T., Sugimoto, M., Nakanishi, E. and Hibi, S. *Polymer* 1993, **34**, 487
11 Swan, P. R. *J. Polym. Sci.* 1962, **56**, 409

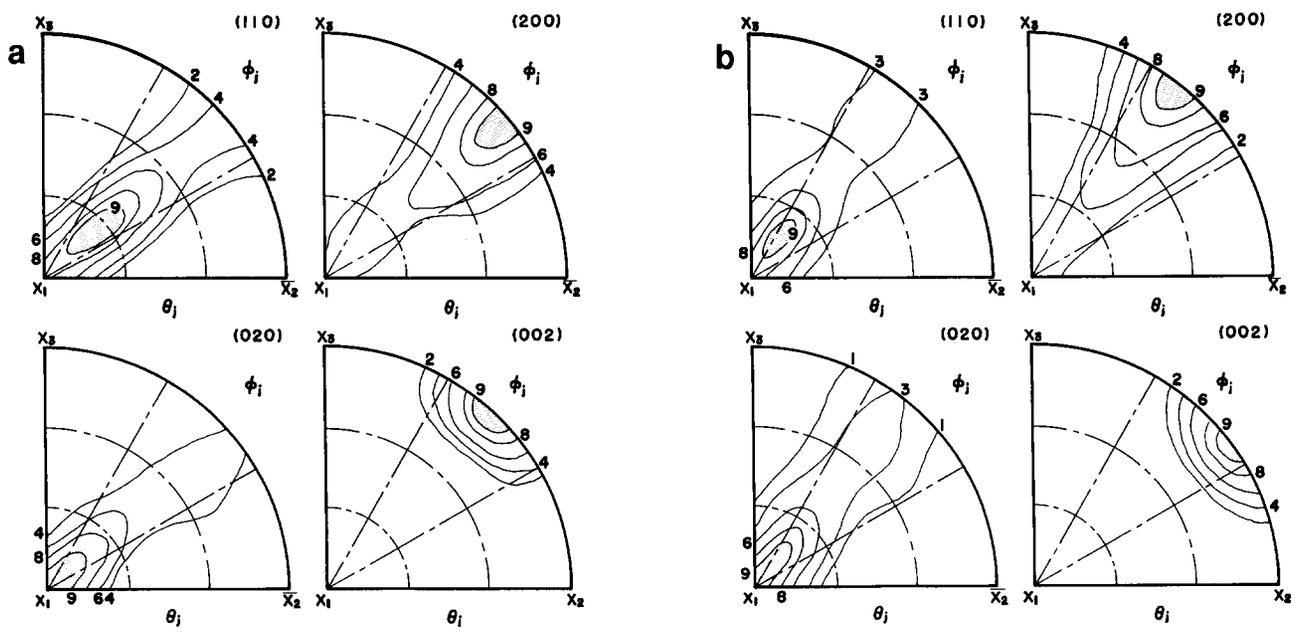

Figure 7 Pole figures calculated from the orientation distribution function by introducing the spiral orientation angle β, the correctional angle δ and the slippage angle α for: (a) condition B; (b) condition C